Functional Molecularly Imprinted Polymer Microstructures Fabricated Using Microstereolithographic Techniques

Peter G. Conrad, II,[*] Peter T. Nishimura,[†] Damian Aherne,[†] Benjamin J. Schwartz,[†] Dongmin Wu,[‡] Nicholas Fang,[‡] Xiang Zhang,[‡] M. Joseph Roberts,[‡‡] and Kenneth J. Shea[*]

[*] Department of Chemistry, University of California, Irvine, Irvine, CA 92697-2025

[†] Department of Chemistry and Biochemistry, University of California, Los Angeles, Los Angeles, CA 90095-1569

[‡]Department of Mechanical and Aerospace Engineering, University of California, Los Angeles, Los Angeles, CA 90095-1569

[‡‡]NAVAIR NAWCWD, Polymer Science and Engineering Branch, China Lake, CA 93555

An ongoing trend in sensing and diagnostics has been miniaturization, the reduction of the size of devices and components to micron or submicron length scales.[1, 2] These small length scales require fabrication methods that are capable of producing spatially resolved, micron-sized features of *functional* materials. Herein, we report the utilization of microstereolithography for fabricating imprinted microstructures capable of recognizing a targeted analyte.

Molecular imprinting is a method for creating cross-linked polymers capable of selective recognition of complex organic molecules.[3-6] Highly selective materials are fabricated by coordinating functional monomers with a desired template molecule

through either covalent bonds or complimentary non-covalent interactions. Polymerization of the complex in the presence of cross-linking monomers results in an insoluble network material. The template is extracted, leaving behind domains that are complementary in size, shape, and functional group orientation to the template molecule.

For imprinted polymers to play a role in microsensors and diagnostic devices, methods must be developed for fabricating molecularly imprinted polymers (MIPs) in two- and three-dimensional patterns. Applications for micro-devices are widespread and include electrophoretic analyses of DNA,[7] implantable medical biosensors,[8] drug screening,[9] and micorelectromechanical systems (MEMS) based instrumentation.[2] Molecularly imprinted sensing devices can be readily integrated with micro-fluidic channels, valves, and pumps.[10] Despite the natural advantages of micro-devices such as high processing speed, high throughput capabilities, minimal sample consumption, simple integration of components for sample preparation and analysis, and low manufacturing costs, there has been only a limited number of reports of successfully micropatterend and functional molecularly imprintable polymers.[11] Logical approaches for producing micro-patterned, imprintable polymers would include micro-contact printing (soft lithography).[11-13] microstereolithography (μSL) and 2 photon 3D lithography.[14]

Herein, we report the successful combination of μSL techniques with molecular imprinting to create functionalized, three-dimensional microstructures. In particular, we demonstrate adenine recognition in well-defined, micron-sized structures, a system we chose for the biological significance of synthetic receptors capable of nucleotide recognition.[15] This selectivity was achieved using 9-ethyl adenine (9-EA, **1**) as the

imprint molecule and methacrylic acid (MAA, **2**) as the functional monomer.[16] The photopolymerizable solutions also contain benzoin ethyl ether (BEE, **3**), chosen as the photoinitiator because of the favorable overlap between its absorption maximum and the laser excitation wavelength of our μSL set-up, and trimethylolpropane trimethacrylate (TRIM, **4**), used as the cross-linker. Polymer microstructures imprinted with 9-EA display an affinity for rebinding a fluorescent analog, 9-dansyl adenine (9-DA, **5**), while microstructures fabricated in the absence of 9-EA showed substantially lower affinity for the fluorescent derivative.

Insert Figure 1.

Microstereolithography (μSL) is a method for manufacturing complex three-dimenstional shapes, by means of localized photopolymerization via a sharply focused laser beam.[17] μ SL was first reported in 1993 utilizing principles based on stereolithography to fabricate macro-sized models.[18] A CAD program is used to horizontally slice the desired three-dimensional image into two-dimensional layers. A directed UV laser beam is focused to 1-2 μm onto the surface of a glass microscope slide coated with a thin layer of a liquid monomer solution, resulting in localized photopolymerization; synchronized motion of the substrate in the x-y plane is then used to fabricate the pattern of the lowest two-dimensional slice.[17, 19] Translation along the z-axis allows the next layer to be written on top of the first. Repetition of these steps allows complex and intricate microstructures to be built in a layer-by-layer fashion.

The fact that polymerization takes place on the desired micro-scale in the *x-y* plane results directly from the tight focus of the photolithographic lasers used for μSL. To achieve spatial resolution in the third dimension, however, the photopolymer

formulation must have a high enough absorbance at the excitation wavelength to control the depth that the light penetrates into the sample, which in turn determines the height, or "curing depth", of each of the polymerized layers. Jacobs *et al.* [20] have established a working curve for controlling curing depth in μSL based on the photopolymer's threshold exposure:

$$C_d = D_p \ln(E/E_c), \qquad \textbf{Eq. 1}$$

where C_d is the curing depth, E and E_c are the laser power and threshold power for polymerization to occur, respectively, and D_p is the penetration depth of the laser into the solution, defined via the Beer-Lambert law as:

$$D_p = 1/\{2.3(\varepsilon_I[I] + \varepsilon_{UVA}[UVA])\}, \qquad \textbf{Eq. 2}$$

where ε_I is the molar extinction coefficient of the initiator, [*I*] is the initiator concentration, ε_{UVA} is the molar extinction coefficient of the UV absorber, and [*UVA*] is the UV absorber concentration. Tinuvin, **6**, has a large molar absorptivity coefficient (151,600 mol^{-1} cm^{-1}) at 364 nm (the photopolymerization wavelength we employed) and was found to be an effective UVA to achieve low curing depths (high *z* spatial resolution).

One of the major questions we address here is whether or not the process of producing the desired 3-D pattern via μSL, including the photopolymerization conditions and the addition of Tinuvin, is compatible with maintaining the performance of the molecularly imprinted polymer. The evaluation of rebinding selectivity of imprinted polymers is traditionally conducted using HPLC techniques. However, the theoretical number of binding sites in the small amounts of micropatterned polymer generated by μSL techniques is below the detection limits for HPLC analysis. An attractive alternative

is to utilize the emission of a fluorescently-tagged analyte to evaluate the binding sites created during the imprinting process within a microfabricated structure. A microstructure that has a higher capacity to rebind an analyte will have a higher fluorescent intensity.

Thus, to obtain a fluorescence assay based on our MAA/adenine polymer/template system, adenine was derivatized at the 9- position using dansyl chloride, yielding fluorescent 9-dansyl adenine (9-DA, **5**).[21] The primary binding interactions between adenine derivatives and carboxylic acid functional groups are believed to be Watson-Crick and Hoogstein H-bonding interactions.[16] These recognition elements allow a fair degree of freedom in substitution at the 9-position while maintaining overall adenine specificity by the MIPs. It is assumed that the size of the dansyl group will not appreciably affect the rebinding of 9-DA.

Insert Figure 2.

To establish that our choice of BEE as a photoinitiator and Tinuvin as a UV absorber do not interfere with the imprinting process or create additional non-specific binding interactions, we prepared a variety of non-patterned test samples under different conditions. Table 1 summarizes the proportions of reagents used to generate the photopolymerizable MIP solutions; each of the four solution mixtures (**S1-S4**) was dip-coated onto glass microscope slides previously silylated with 3-(trimethyoxysilyl)propyl methacrylate, allowing for better adhesion of the photodeposited polymer to the glass substrates.

Insert Table 1.

The polymers were then grown by light exposure in a UV chamber for 5 minutes and then washed in chloroform for 12h to remove 9-EA**,** Tinuvin, BEE and any unreacted monomers. These unpatterned samples were then bathed in a 1 x 10^{-5} M chloroform solution of 9-DA. The 9-DA absorbed in the samples was excited using the 488 nm line from an Ar^{+} laser (a wavelength chosen to avoid absorption by any residual Tinuvin), and ~600 nm dansyl fluorescence from the samples was imaged through a 530 nm long pass filter onto a CCD camera. Integration of the fluorescent image was plotted as a function of time (Figure 3). The rebinding ability of the imprinted polymers is reflected in the intensity of the fluorescence associated with each polymer.

To investigate rebinding, the total emission intensity obtained by spatial integration over the entire image of each sample is plotted as a function of time of exposure to the 9-DA analyte solution in Figure 3. Inspection of Figure 3 reveals that the uptake of 9-DA for all four samples reaches saturation within 25 minutes, the first data point taken. The uptake of 9-DA in the MIP (polymerized in the presence of the 9-EA template, diamonds and squares) is significantly greater than in the control polymers (polymerized without the template, circles and triangles), providing the desired affinity. The data also show that Tinuvin has a minimal affect on the imprinting process: both the MIPs (fabricated from solutions **S1** and **S2** containing the 9-EA template) and control samples (fabricated from solutions **S3** and **S4** without the template) behaved similarly whether Tinuvin was added to the mixture (squares and triangles) or not (circles and diamonds). In addition to the fact that Tinuvin does not adversely affect the polymer affinity, additional (qualitative) rebinding experiments confirmed that changing the

initiator does not affect the imprinting process or the subsequent polymer rebinding behavior.

Insert Figure 3.

Having established that formulating the functional polymer solutions for patterning via μSL does not interfere with the imprinting or selectivity of the resulting polymer, we next devoted our attention to the micropatterning of functional polymers via μSL. For the first experiments simple, two-dimensional patterns were fabricated to verify that the patterned microstructures show similar selectivity to the bulk polymers. Two-dimensional grids were fabricated from the UV-curable MIP and control UV curable solutions (**S1** or **S3**, respectively) using the 364 nm line of the Ar^+ laser and an x-y-z motorized stage. Figure 4 shows an image of the resulting pattern, which has an overall dimension of 600 μm × 600 μm; the width of the lines comprising the grid is ~20 μm. In other experiments we were able to produce features as small as a few μm.

Insert Figure 4.

After fabrication, the micro-patterned polymers were gently washed in isopropyl alcohol and then chloroform. Uptake studies were performed by bathing both the imprinted and control structures in 9-DA chloroform solutions (1.8×10^{-4} M) and measuring the total fluorescence from each sample as a function of time. The 2-D patterned MIP showed a 5:1 preference for 9-DA over the control polymer, a value comparable to previous reports for 9-EA MIPs prepared under bulk conditions.[16]

With the success of 2-D patterned MIPs, the next step was to produce functional 3-D structures. As discussed above, the curing depth, Eq. 1, determines the z-resolution achievable for 3-D structures fabricated by μSL. Based on the height of the 2-D

structures shown in Figure 4 and the concentration and absorptivity of Tinuvin, we estimated that the curing depth of the polymerization solutions was ~20-30 μm. Thus, to fabricate three-dimensional structures, we lowered the *z*-axis of the translation stage by 20 μm after the *x*-*y* scan of each 2-D "slice" was completed. After building up multiple 2-D layers, the resulting three-dimensional polymer objects had a total height of approximately 100 μm; scanning electron micrographs of the 3-D "waffle pattern" produced in this fashion are shown in Figure 5.

Insert Figure 5.

As with the unpatterned and 2-D patterned polymers, rebinding studies were conducted for both the MIP and control 3-D structures. The 3-D structures were rinsed and bathed in chloroform for 12h to wash the 9-EA template and any unreacted materials from the MIP. The structures were then exposed to a solution of 9-DA (1.08×10^{-4} M in chloroform) for increasing time intervals, gently rinsed to remove any residual 9-DA, and fluorescently imaged. The results are shown in Figure 6.

Insert Figure 6.

The significantly diminished fluorescent intensity from the control polymer structure (squares) compared to the imprinted structure (diamonds) indicates that imprinting indeed produces two polymers with significantly different affinities for the target analyte. The rebinding curves also show that the 3-D microstructure is quite sensitive; all the available binding sites become occupied after only ~15 minutes.

In summary, we have demonstrated the ability to fabricate functionalized, three-dimensional molecularly imprinted microstructures using μSL. The experimental conditions used in μSL do not disrupt the binding interactions between the functional

monomers and the template. The range of target analytes that are responsive to molecular imprinting is large and includes simple drugs and their metabolites, pesticides, peptides, and proteins. These techniques will allow the fabrication of functional polymers capable of molecular recognition to be integrated into microfabricated devices.

Acknowledgments: The authors are grateful for DARPA for financial support. Research in the KJS lab is partially supported by the National Institute of Health. BJS is a Cottrell Scholar of Research Corporation, an Alfred P. Sloan Foundation Research Fellow, and a Camille Dreyfus Teacher-Scholar.

Tables and Figures:

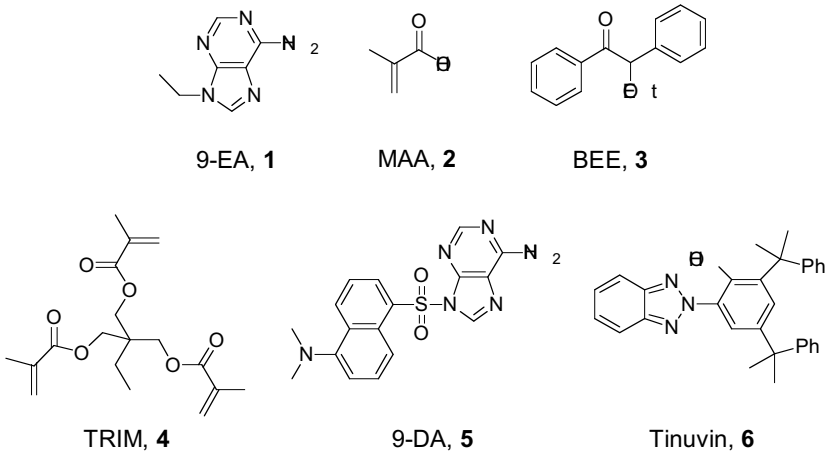

Figure 1. Compounds utilized during the fabrication of MIP structures. 9-Ethyl adenine, **1**, served as the template and methacrylic acid, **2**, was chosen as the functional monomer. Benzoin ethyl ether, **3**, was utilized as the initiator for μSL procedures. TRIM, **4**, was used as a cross-linking agent. 9-Dansyl adenine, **5**, was the fluorescent analog used for the rebinding studies. Tinuvin, **6**, was added as a UV absorber to achieve curing depth resolution.

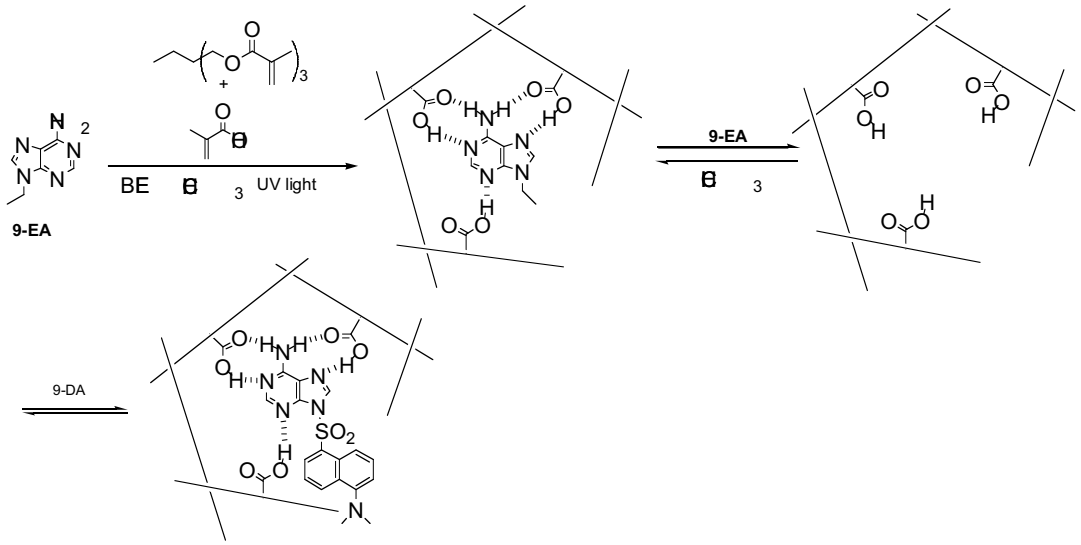

Figure 2. Schematic depicting the fabrication of adenine selective molecularly imprinted polymers based on methacrylic acid. Following removal of the 9-EA template, the imprinted sites selectively bind the fluorescent adenine derivative, 9-DA.

Substrate	**S1**	**S2**	**S3**	**S4**
Chloroform	6.271 g	6.271 g	6.271 g	6.271 g
TRIM	6.274 g	6.274 g	6.274 g	6.274 g
Methacrylic acid	0.327 g	0.327 g	0.327 g	0.327 g
Tinuvin	0.013 g	-	0.013 g	-
Benzoin ethyl ether	0.131 g	0.131 g	0.131 g	0.131 g
9-Ethyl adenine	0.050 g	0.050 g	-	-

Table 1. Composition of solutions used during polymerization procedures.

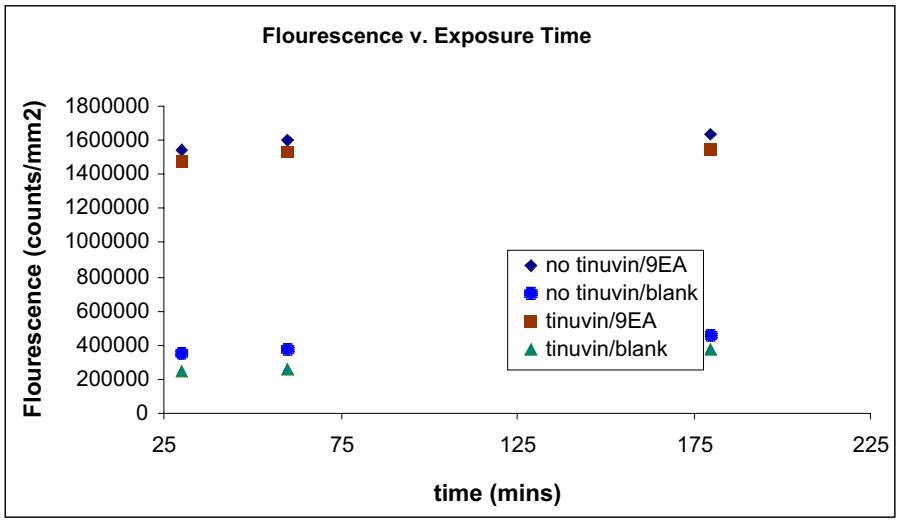

Figure 3. Fluorescence intensity vs time of exposure to 1 x 10^{-5} M chloroform solutions of 9-DA for both 9-EA-imprinted (diamonds and squares) and control (triangles and circles) polymer samples. The results of this rebinding assay indicate that addition of Tinuvin as a UV absorber (necessary for 3-D resolution in μSL) has little effect on the rebinding ability for either the imprinted or control samples.

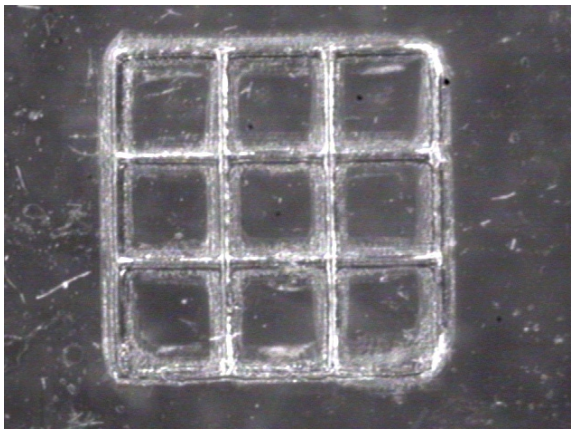

Figure 4. Two-dimensional microstructure (600 μm x 600 μm) fabricated by μSL from solution **S1**.

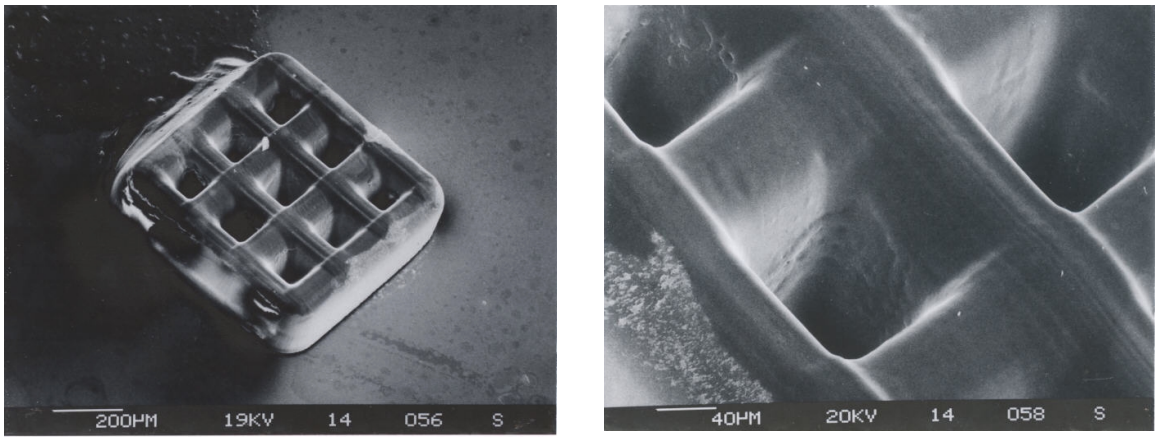

Figure 5. SEM image of a 3-D imprinted microstructure (600 μm x 600 μm x 100 μm). Right: Close-up of the structure shows the wall thickness to be approximately 20 μm.

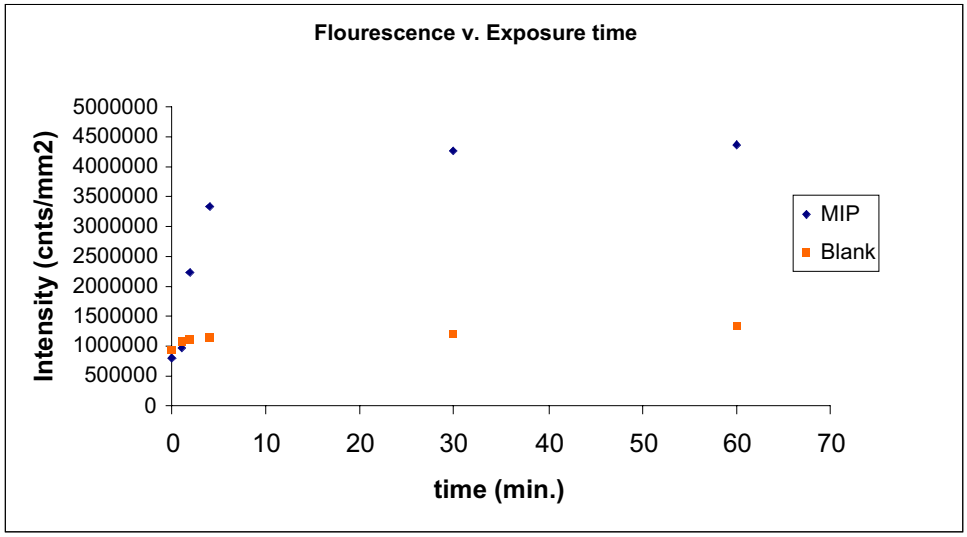

Figure 6. Rebinding isotherm (fluorescence intensity as a function of exposure time to a 1.08 x 10^{-4} M solution of 9-DA in chloroform) for both 9-EA-imprinted (MIP) and control (Blank) 3-D microstructures as those presented in Fig. 5.

[1] X. Zhang, X. N. Jiang and C. Sun, *Sensors and Actuators* **1999**, *77*, 149.
[2] R. Mariella, Jr., *Biomedical Microdevices* **2002**, *4*, 77.
[3] G. Wulff, *Angew. Chem., Int. Ed. Engl.* **1995**, *34*, 1812.
[4] K. J. Shea, *Trends Polym. Sci.* **1994**, *2*, 166.
[5] B. R. Hart, D. J. Rush and K. J. Shea, *J. Am. Chem. Soc.* **2000**, *122*, 460.
[6] K. Haupt and K. Mosbach, *Chem. Rev.* **2000**, *100*, 2495.
[7] G. Yershov, V. Barsky, A. Belgovskiy, E. Kirillov, E. Kreindlin, I. Ivanov, S. Parinov, D. Guschin, A. Drobishev, S. Dubiley and A. Mirzabekov, *Proc. Natl. Acad. Sci. USA* **1996**, *93*, 4913.
[8] Z. A. Strong, A. W. Wang and C. F. McConaghy, *Biomedical Microdevices* **2002**, *4*, 97.
[9] Y. Jiang, P. Wang, L. E. Locascio and C. S. Lee, *Anal. Chem.* **2001**, *73*, 2048.
[10] K. Ikuta, K. Iketa, A. Takahashi and S. Maruo, "Artificial Cellular Device with Cell-Free Protein Synthesis Ability Constructed by Chemical IC Chips", presented at *Proceedings of the 2001 1st IEEE Conference on Nanotechnology 2001*, Piscataway, NJ, **2001**.
[11] M. Yan and A. Kapua, *Anal. Chim. Acta.* **2001**, *435*, 163.
[12] G. M. Whitesides, E. Ostuni, S. Takayama, X. Jiang and D. E. Ingber, *Annu. Rev. Biomed. Eng.* **2001**, *3*, 335.
[13] G. Vozzi, C. J. Flaim, F. Bianchi, A. Ahluwalia and S. Bhatia, *Materials Science and Engineering C* **2002**, *20*, 43.
[14] G. Witzgall, R. Vrijen, E. Yablonovitch, V. Doan and B. J. Schwartz, *Opt. Lett.* **1998**, *23*, 1745.
[15] K. J. Shea, D. A. Spivak and B. Sellergren, *J. Am. Chem. Soc.* **1993**, *115*, 3368.
[16] D. A. Spivak, M. A. Gilmore and K. J. Shea, *J. Am. Chem. Soc.* **1997**, *119*,
[17] E. Manias, J. Chen, N. Fang and X. Zhang, *Appl. Phys. Lett.* **2001**, *79*, 1700.
[18] K. Ikuta and K. Hirowatari, *Proc. IEEE Micro Electro Mech. Syst.* **1993**, 42.
[19] X. N. Jiang, C. Sun, X. Zhang, B. Xu and Y. H. Ye, *Sensors and Actuators* **2000**, *87*, 72.
[20] P. F. Jacobs, in *Rapid Prototyping and Manufacturing: Fundamentals of Stereolithography*, Society of Manufacuring Engineers **1992**.
[21] *Synthetic Procedures in Nucleic Acid Chemistry*, Vol. 1 and 2 (Eds: W. W. Zorbach and R. S. Tipson), Interscience **1968**.